Available online at www.sciencedirect.com

ScienceDirect

Energy Procedia 77 (2015) 21 – 28

Energy Procedia

5th International Conference on Silicon Photovoltaics, SiliconPV 2015

FFE IBC cells: impact of busbars on cell performance with circuit modelling

Antonius R. Burgers, Nicolas Guillevin, Agnes A. Mewe, Aishwarya Suvvi, Pierpaolo Spinelli, Arthur W. Weeber, Ilkay Cesar

ECN Solar Energy, PO Box 1, NL-1755 ZG Petten, The Netherlands

Abstract

IBC cells with Front Floating Emitter (FFE) pose different design challenges compared to more conventional IBC cells with FSF (Front Surface Field). The FFE enables hole transport over distances that are large compared to the typical BSF or emitter width. The core of the cell design is commonly a device simulation in which, because of the computer resources involved, typically one simulates an as small as possible, but representative part of the solar cell. In an IBC cell this corresponds to ½ of the BSF and ½ of the emitter. Such a unit cell does not account for important geometric features, such as busbars and pads, edges or interruptions in metallization fingers.

We show how to construct an equivalent circuit for our Mercury FFE IBC cells to model features beyond the unit cell efficiently, taking into account the lateral hole transport in the FFE. We show how its predictions can be correlated with voltage maps of the FFE voltage, and used for optimum design of for instance busbars.

The highest efficiency of our Mercury FFE IBC cells to date is 20.9% with a short-circuit current of 41.3 mA/cm^2, obtained with screen printed contacts.

© 2015 The Authors. Published by Elsevier Ltd. This is an open access article under the CC BY-NC-ND license (http://creativecommons.org/licenses/by-nc-nd/4.0/).

Peer review by the scientific conference committee of SiliconPV 2015 under responsibility of PSE AG

Keywords: silicon solar cell; modeling; circuit simulation; Front Floating Emitter

1. Mercury FFE IBC cells

IBC (interdigitated back contact) cell technology is ideal for high-efficiency solar cells mainly because all metallization can be applied to the rear side of the cell which eliminate shading losses. Although IBC solar cells have been shown to yield very high conversion efficiencies [1], cost effective production of these devices poses challenges. To allow all contacts to be applied to the rear of the cell, the rear collecting junction (the emitter) is interrupted by a non-collecting junction (the BSF) as illustrated in Figure 1. Therefore, any carrier that is photo-

1876-6102 © 2015 The Authors. Published by Elsevier Ltd. This is an open access article under the CC BY-NC-ND license (http://creativecommons.org/licenses/by-nc-nd/4.0/).
Peer review by the scientific conference committee of SiliconPV 2015 under responsibility of PSE AG
doi:10.1016/j.egypro.2015.07.005

generated above a BSF area needs to travel laterally to an emitter area. If the BSF regions become too wide, the collection probability of carriers generated above the BSF will decrease: an effect referred to as electrical shading [2]. To prevent loss in cell performance due to electrical shading for an FSF IBC cell, the typical width of the BSF is in the order of 0.2-0.4 mm out of a typical cell pitch of 1.5 mm.

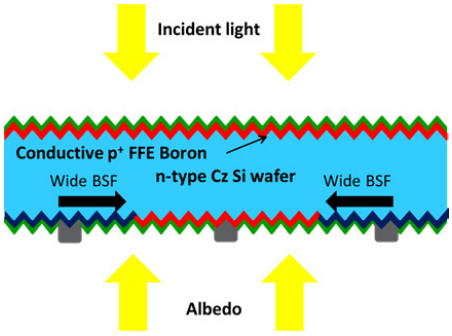

Figure 1: Cross-section of the Mercury cell; a bifacial n-IBC solar cell with screen-printed contacts.

The inequality of BSF and emitter widths results in strict patterning tolerances for processing but also has implications for the metallization [3]. For instance for PVD metallization the BSF fingers will be narrow compared to the emitter fingers. Either the metallization has to be thick to achieve sufficient conductivity also on the BSF, or the BSF metallization has to be partially deposited on the emitter, making sure there is sufficient isolation between BSF metallization and emitter. Equal widths of both polarities would allow one to metallize the IBC cell with blanket metallization technologies such as PVD and plating without the need of an isolation layer. This is a significant opportunity for process simplification and cost reduction. To allow for wider BSF regions we have introduced the Mercury IBC cell [3]: an IBC cell with a conductive Front Floating Emitter (FFE). In fact back contact FFE cells have been proposed before, e.g. in [4, 5] but have not become a main stream technology.

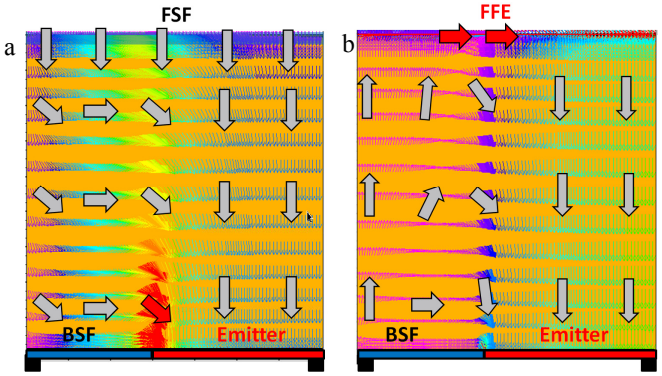

Figure 2: Current vector plots from 2D numercial device simulations (Atlas), showing the hole current flow over the cross-section of an IBC cell either with (a) FSF or (b) FFE. The big arrows indicate the overall current flow direction and the red arrows indicate the largest current densities.

Figure 2 compares the flow of holes in a unit cell consisting of ½ a BSF and ½ an emitter for both the FSF and FFE case. In the FSF case the photogenerated holes in the base over the BSF need to be collected laterally by the nearest emitter. The transport requires a concentration gradient in the holes, and hence the carrier concentrations above the BSF become high when the BSF is wide, leading to recombination. In the FFE case the hole current flow is completely different. The photogenerated holes over the BSF are collected in the FFE, then transported as majority carriers through the FFE to the FFE above the rear emitter, where they are re-injected for subsequent collection by the rear emitter. Effectively the holes are pumped from the BSF region to the emitter contact.

The pumping effect in this way increases the transport length for holes generated above the BSF, allowing the BSF width to be as wide as the emitter width without significant loss in cell efficiency. With proper tuning, the FFE can be applied as an effective means to increase the BSF width with marginal loss in cell performance while assuring process simplification and cost reduction. Besides this, the design leads to more freedom in the interconnection lay-out and increases the tolerances for the module fabrication.

Full area 6'' screen printed mercury IBC cells have been made using a process based upon ECN's n-pasha screen printed process for n-PERT cells [6] and reported in several of our papers. The highest efficiency achieved to date is 20.9% with an short-circuit current of 41.3 mA/cm^2 (in-house measurement, mismatch corrected, not independently confirmed) illustrating the effectiveness of the FFE passivation.

2. Voltage maps of the FFE

The FFE plays a major role in the lateral carrier transport. Hence it can be useful to know more about its voltage.

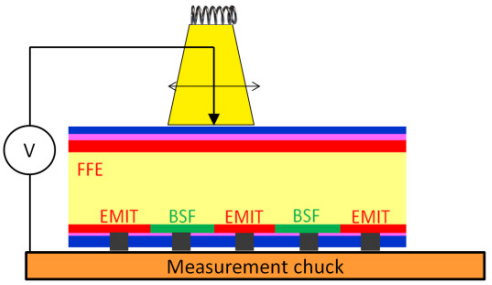

Figure 3: Mapping the FFE voltage relative to the rear side metallization with the corescan.

Figure 3 shows how the Sunlab® corescan instrument [7] can be used to conveniently map the FFE voltage. The IBC cell is mounted on the chuck, the BSF and emitter contacts are shorted by the chuck. The instrument features a white light source with a beam diameter of about 1 cm. In the center of the beam there is voltage probe, sensing the FFE voltage relative to the chuck. The light beam together with the voltage probe is scanned across the wafer, resulting in a map of the FFE voltage. When evaluating the maps we need to keep in mind that because of the local illumination used in the FFE voltage map, holes might leak laterally to outside of the spot, leading to less charging of the FFE, resulting in a lower FFE voltage than would occur in a cell operating in full area illumination.

3. FFE voltage maps.

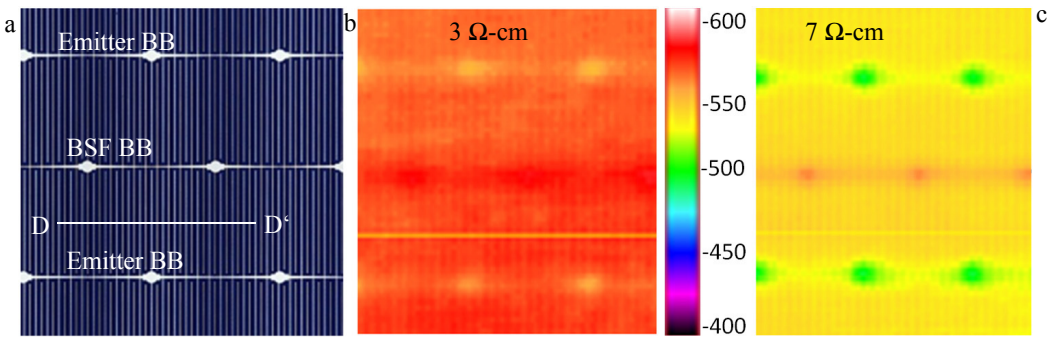

Figure 4: (a) optical picture of rear side of cell, and (b) and (c) voltage scans (mV) of the FFE at the front side. The horizontal yellow line is an artefact.

The IBC cells feature an interdigitated pattern on the rear side, as shown in Figure 4a. The BSF and emitter fingers are connected to the BSF and emitter busbars respectively. The busbars for both polarities conduct the current to contact pads. The contact pads allow for measuring the cell on a chuck. More importantly they allow for easy interconnection and encapsulation of IBC cells in a module. The pads serve to mount the cell on a conductive patterned foil for instance with conductive adhesives [8].

Figure 4b and Figure 4c show examples of FFE voltage scans. The cells in this case feature a 1 mm wide BSF, as well as a 1 mm wide emitter. Despite the metallization being at the rear side of the cell, the features in FFE voltage maps at the front side of IBC FFE cells are clearly correlated with the rear side metallization of the cell.

- The BSF busbars are visible as areas of higher voltage. In particular the wider pads of the busbars are well recognizable.
- The emitter busbars are well visible as well, however as areas of lower voltage, in particular above the wider pad areas.
- The finger pattern is clearly visible, with the voltage higher above the BSF fingers, lower above the emitter fingers.

In the p-type FFE the majority carriers holes flow from high to low voltage:

$$\overrightarrow{J_h} = \vec{\nabla} V_{FFE}$$

The fact that the voltage is high above the BSF fingers, and low above the emitter fingers, implies that current is flowing through the FFE from above the BSF to above the emitter, providing direct evidence of the pumping effect in progress. The FFE voltage is high above the BSF busbars and in particular above its pads, so there is a net hole current flow away from above the busbar and its pads. The source of this current is the collection of holes by the FFE from the base. The FFE voltage is low above the emitter busbars and in particular above its pads, so there is a net hole current flow towards the busbar and its pads. The sink of this current is the injection of holes from the FFE into the base and their subsequent collection by the rear emitter.

The effects of the pads on the FFE voltage is noticeable over significant distances, certainly larger than the pad diameter.

4. Mercury cells and their equivalent circuit

In a device simulation, typically one simulates a unit cell as indicated in Figure 5a. Figure 5b shows the type of equivalent circuit we used, superimposed upon a schematic of the FFE IBC cell. The pink areas denote the p-type doped (emitter and FFE) regions, the blue areas the n-type doped (base and BSF) regions.

The wires and resistors represent majority carrier transport, electrons in base and BSF, holes in FFE and rear emitter. Minority carrier transport and junctions are modelled within the non-linear circuit elements, i.e. the diodes and transistors. The illuminated diodes represent the base-FFE junction above the BSF, as in a normal p-n junction solar cell. The illuminated transistors represent the emitter-base-FFE parts of the IBC cell. For the FFE-base-emitter to operate as a transistor, the requirement is that the minority carriers must be able to cross the base, e.g. their diffusion length L_h must be larger than the thickness w of the wafer. This condition must be satisfied in any IBC cell, because carriers generated at the front side must be able to diffuse to the junction at the rear side. If not, the current of the IBC cell would be unacceptably low. Equivalent circuits for FFE type back contacted cells employing transistors have been proposed before in for instance [5, 12].

Units such as these can be connected together using the nodes FL, FR, BL, BR and ER. Here L and R are an abbreviation for left and right, F, B, E for FFE, base and emitter respectively.

For the transistors we use a basic Ebers-Moll model. Main parameters of the Ebers-Moll model are the transistor gain, and its dark current. The gain is directly related to the ratio L_h/w. The larger this ratio is, the higher the probability that a carrier injected by the FFE into the base at the front side can be collected by the rear side junction. The process occurs in the reverse direction too. As the cell is biased towards higher voltages, the rear emitter will inject carriers into the base, for subsequent collection by the FFE.

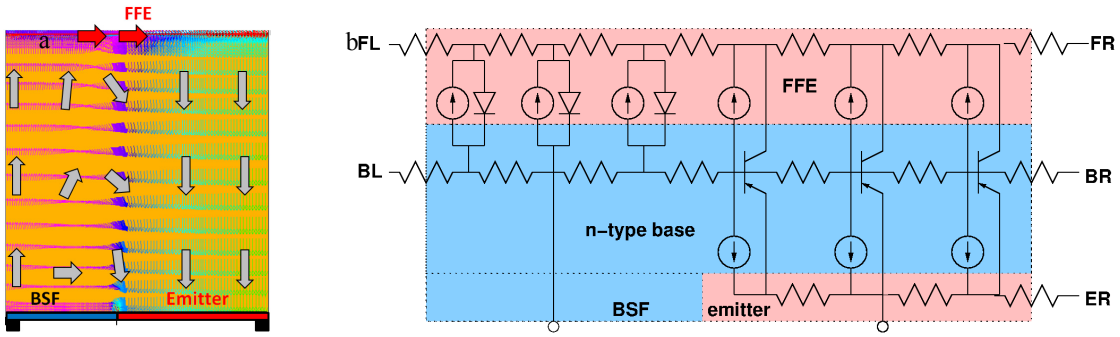

Figure 5: (a) unit cell for device simulation, (b) sample equivalent circuit used for unit cell.

In literature, circuit simulation to model a cell beyond the basic unit cell has been described before, for instance [10, 11]. What these approaches have in common is that device simulation is used to simulate different representative parts of the cell. The results of these device simulations are summarized as a 2-diode equivalent circuit. This is a 2-terminal circuit. This approach is justified if there are no significant current flows into or out of the unit cell in addition to the current flows through the contacts. In the case of the mercury IBC cell the FFE allows current flows of the same order of magnitude as through the contacts over relatively large distances. A two terminal equivalent circuit is therefore usually not good enough in our case.

5. Circuit simulation and FFE voltage scans.

We perform circuit simulations in a 1-D geometry. The reference case A corresponds to a simulation along the line D-D' in Figure 4a, representing the characteristics of several unit cells. The effects of both the BSF and emitter busbar and pad areas are simplified in the model by positioning them parallel to the fingers of the unit cell, in contrast to the real cell structure with perpendicular orientation. Thus these busbars and pads are simply simulated as wide BSF or emitter regions on either side of the unit cell structures. This structure should give insight in the first order effects that play a role in the device. Future effort is directed to develop a 2D structure that accurately represents the cell geometry. The exact structure simulated is depicted in Figure 6. For the reference case A we simulate 4 ½ BSF units and 4 ½ emitter units, where a single BSF or emitter has width of 1 mm. The busbars are modeled as a wide BSF region (Figure 6a, case B) or emitter region (Figure 6b, case C) with a ½ width of 1.5 mm. All 3 cases A,B and C are simulated for both 3 and 7 Ω-cm bulk resistivity. The I-V parameters can be found in Table 1.

Table 1: I-V parameters of circuit simulations

case	R_{bulk}	J_{sc}	V_{oc}	FF	eta
	Ω-cm	mA/cm^2	mV	%	%
A: reference	3	39.62	649.8	82.2	21.15
B: 1.5 mm BSF	3	38.84	649.8	81.7	20.62
C: 1.5 mm emitter	3	39.87	649.8	79.2	20.51
A: reference	7	39.88	649.8	81.3	21.08
B: 1.5 mm BSF	7	39.28	649.8	80.9	20.65
C: 1.5 mm emitter	7	40.14	649.8	75.9	19.78

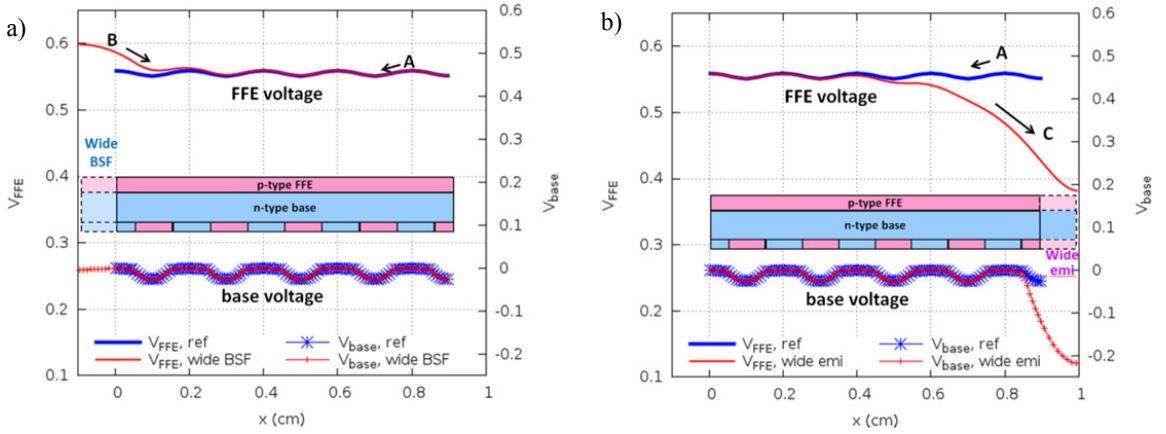

Figure 6: Simulated FFE and base voltage for (a) BSF busbar and (b) emitter busbar (at short circuit conditions, 7Ω-cm). A: ref, B: wide BSF, C: wide emitter.

The same reference case A is plotted in both Figure 6a and b. In case A we observe a characteristic ripple in the FFE voltage correlated with the rear diffusion pattern. Over the BSF diffusions there is high voltage, over the emitter diffusion a low voltage. This voltage difference is induced by the pumping current. The same ripple is observed in the FFE voltage scans and provides experimental evidence of the pumping effect.

Over the BSF busbars (Figure 6a), holes collected in the FFE have to be pumped over a larger distance to the closest emitter contact. Since a larger hole current is flowing laterally through the FFE, over a larger distance than in the unit cell, a higher FFE voltage above the BSF busbars results. As a consequence, the base-FFE junction over the BSF busbars moves towards open circuit, which reduces the collection probability of the carriers. This translates to some electrical shading, as can be observed from the somewhat lower current density for case B in Table 1.

Over the emitter busbars, electrons need to travel laterally in the base to the nearest BSF contact. This induces a drop in the base voltage over the rear emitter. For a 7 Ω-cm 150 um thick wafer the sheet resistance of the base (at low injection) is about 470 Ω/□. Hence over relatively short distances significant voltage drops can be sustained. The voltage drop in the base increases the forward biasing of the base-FFE junction over the rear emitter. Hence carriers are more effectively injected into the base over the rear emitter: the cell operates almost as if there was a via as in an Emitter Wrap Through (EWT) solar cell. The flow of holes in the FFE towards the wide emitter busbar is associated with a voltage gradient in the FFE. However due to the relatively high conductivity of the FFE (~70 Ω/□) compared to the base, the voltage in the FFE is affected over a larger distance than in the base.

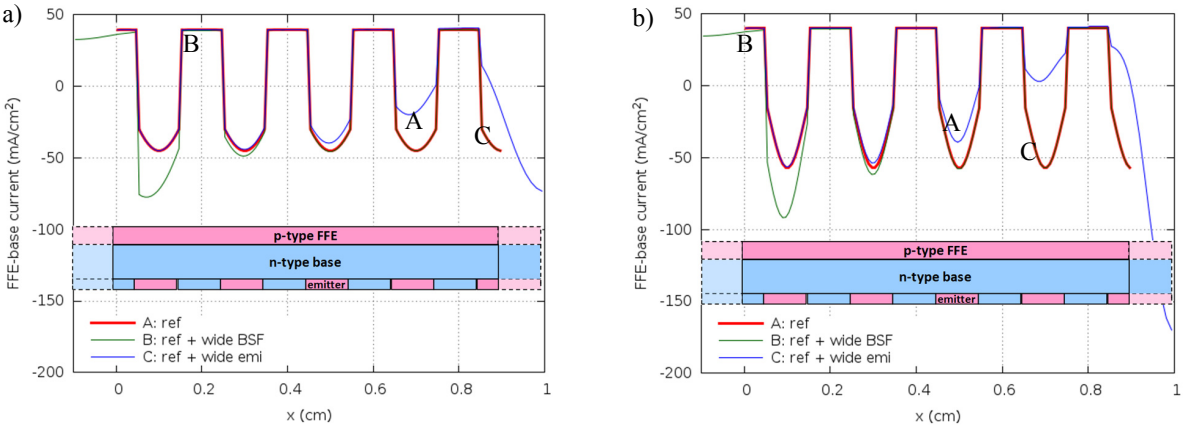

Figure 7: FFE-base junction current density for (a) 3 Ω-cm, (b) 7 Ω-cm base resistivity. A: ref, B: wide BSF, C: wide emitter.

In Figure 7 the current density across the FFE-base junction is plotted (at short circuit conditions). It can be observed that over the BSF regions the current is positive (being collected by the FFE), over the emitter regions the current is negative, and being injected from the FFE into the base.

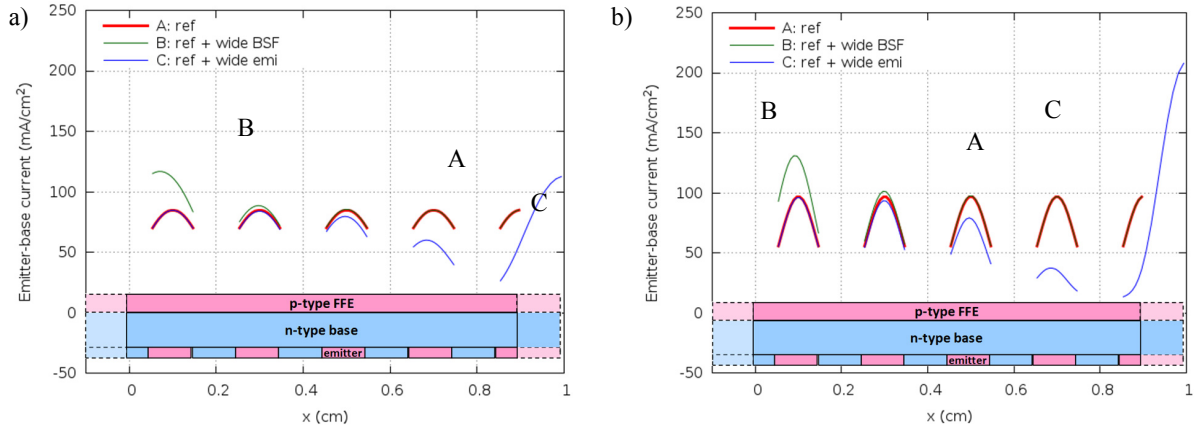

Figure 8 Current density at the base-emitter junction at the rear side (a) 3 Ω-cm, (b) 7 Ω-cm base resistivity. A: ref, B: wide BSF, C: wide emitter.

In a low resistivity wafer the voltage effects in the base become smaller, and the pumping effect for holes is less pronounced. This can be seen in Figure 8 where the emitter-base junction current is plotted (at short circuit conditions). Since in this case the BSF is as wide as the emitter, the current density at the rear junction is roughly twice the cell short circuit density. For the 7 Ω-cm case the emitter-base junction current over the wide emitter increases to values over 200 mA/cm^2, whereas for the emitter-base junction next to the wide emitter the current density drops to a small value. For the 3 Ω-cm case similar effects occur, but they are less pronounced.

The enhanced current transport to wide emitter areas has potential consequences for the rear pattern design too. Current is directed in the FFE towards the pads. The pads hence attract current directly, and less current is transported through the emitter busbars and fingers around the pad. So there is room to use less metal for those parts of the metallization.

6. Conclusions and outlook

The FFE voltage scan is an easy to use and telling diagnostic for the FFE IBC cell. The resulting voltage map can well be linked to the cell geometry. The current flow through the FFE can be derived from the voltage map.

Equivalent circuit techniques provide an effective means to model effects beyond unit cells and reveal the physics at work at the bus bars, and explain FF and current effects. The lateral currents in the base and FFE are associated with voltage gradients in FFE and base. They have the effect of moving the base-FFE junction towards higher forward bias. Over the rear emitter this has the effect of enhancing the re-injection of holes into the base, enhancing the pumping effect. Over the BSF this has the effect of less effective carrier collection into the FFE, resulting in electrical shading.

The circuit simulation results we have shown in this paper have limitations in making quantitative statements for our actual cell. Work is underway to extend the equivalent circuit to 2-D networks to be able to quantify effects more precisely.

The authors gratefully acknowledge the support of the Dutch Ministry of Economic Affairs, within the TKI framework, project IBChampion.

References

[1] Smith et al. SunPower's Maxeon Gen III solar cell: High Efficiency and Energy Yield", Proc. 39th IEEE PVSC, Tampa, 2013
[2] Hermle M, et al. Shading Effects in Back-Junction Back-Contacted Silicon Solar Cells. Proc. 33rd IEEE Photovoltaic Specialists Conference, San Diego, CA, 2008.
[3] Cesar I, Guillevin N, Burgers AR, Mewe AA, Koppes M, Anker J, Geerligs LJ, Weeber AW. Mercury: A back junction back contact front floating emitter cell with novel design for high efficiency and simplified processing. Energy Procedia.2014;55:633 – 42
[4] Gutiérrez R, Hernando F, Jimeno JC, Uriarte S. Industrial manufacturing process of silicon TWT solar cell. Proc. 19th EU PVSEC, Paris, 2004
[5] Sah C et Al. Floating Emitter Solar Cell, US patent 4,665,277, 1987.
[6] I.G. Romijn IG et Al. Industrial Cost Effective N-Pasha Solar Cells with >20% Cell Efficiency, Proc. 29th EU PVSEC, Amsterdam, 2014
[7] van der Heide, ASH; Bultman, JH, Hoornstra, J, Schönecker, A. Error diagnosis and optimisation of C-Si solar cell processing using contact resistances determined with the Corescanner, Solar Energy Materials & Solar Cells (Elsevier), 2002;43:p.43-.
[8] de Jong PC et Al. Progress made with back-contact modules using conductive adhesive interconnection technology. Proc. 22nd EU PVSEC, Milano, 2007
[9] Ebers JJ, Moll JL. Large-signal behavior of junction transistors. Proceedings of the Institute of Radio Engineers, 1954;42:1761–1772.
[10] Magnone P, Debucquoy M, Giaffreda D, Niels Posthuma N, Fiegna C. Understanding the influence of busbars in large-area IBC solar cells by distributed SPICE Simulations IEEE J. Phot, 2015;5:552-8
[11] Fell A, Fong KC, McIntosh KR, Franklin E, Blakers AW. 3-D simulation of Interdigitated-Back-Contact silicon solar cells with Quokka including perimeter losses IEEE J. Phot, 2014;4:1040-4
[12] Jimeno JC, Uriarte S, Ikaran C, Nafarrate R, Barbazán N, Petrina I. Modeling the TWT structure. Proc. 19th EU PVSEC, Paris, 2004